On the crystal structure of the ordered vacancy compound $Cu_3In_5\square Te_9$

G.E. Delgado[a,*], C. Rincón[b], and G. Marroquín[c]
[a]*Laboratorio de Cristalografía, Departamento de Química, Facultad de Ciencias, Universidad de Los Andes, Mérida 5101, Venezuela.*
**e-mail: gerzon@ula.ve*
[b]*Centro de Estudios de Semiconductores, Departamento de Física, Facultad de Ciencias, Universidad de Los Andes, Mérida 5101, Venezuela.*
[c]*Escuela Superior de Ingeniería Química e Industrias Extractivas, Instituto Politécnico Nacional, Zacatenco 07738, Ciudad de México, México.*

Received 4 November 2018; accepted 20 November 2018

The crystal structure of the ordered vacancy compound (OVC) $Cu_3In_5\square Te_9$ was analyzed using powder X-ray diffraction data. Several structural models were derived from the structure of the Cu-poor Cu-In-Se compound β-$Cu_{0.39}In_{1.2}Se_2$ by permuting the cations in the available site positions. The refinement of the best model by the Rietveld method in the tetragonal space group $P\bar{4}2c$ (N° 112), with unit cell parameters $a = 6.1852(2)$ Å, $c = 12.3633(9)$ Å, $V = 472.98(4)$ Å^3, led to $R_p = 7.1$ %, $R_{wp} = 8.5$ %, $R_{exp} = 6.4$ %, S = 1.3 for 162 independent reflections. This model has the following Wyckoff site atomic distribution: Cu1 in $2e$ (0,0,0); In1 in $2f$ (1/2,1/2,0), In2 in $2d$ (0,1/2,1/4); Cu2-In3 in $2b$ (1/2,0,1/4); $\square$ in $2a$ (0,0,1/4); Te in $8n$ (x, y, z).

Keywords: Semiconductors; ordered vacancy compound; crystal structure; X-ray powder diffraction; Rietveld refinement; $CuInTe_2$

PACS: 61.05.cp; 61.50.Nw; 61.66.Fn; 61.40.b

DOI: https://doi.org/10.31349/RevMexFis.65.360

1. Introduction

From the analysis of the phase diagrams of $I_2VI-IV_2VI_3$ pseudo-binary systems (where I = Cu or Ag; III = Ga or In; and VI = S, Se or Te), the formation of the $I_3-III_5-VI_9$ ternary semiconducting compounds has been shown [1]. The chemical formula of these materials, which have a deficiency of one cation over the anions, can be written as $I_3-III_5-\square-VI_9$ where $\square$ represents the cation vacancy. Also, the existence and stability of these $I_3-III_5-VI_9$ compounds can also be explained [2] as due to the presence in I-III-VI_2 chalcopyrite structure compound of interacting ($III^{+2}I + 2V^{-1}I$) donor-acceptor defect pair which is electrically inactive and thus, do not contribute to the total charge carriers. For these reasons, they are known as Ordered Vacancy (OVC's) or Ordered Defect Compounds (ODC's). The semiconducting behavior of these OVC's has been explained, based on the four electrons-per-site rule, by assigning to this vacancy a zero valent atom [3].

Some compounds of the $Ag_3III_5VI_9$-type, as for example $Ag_3Ga_5Se_9$, $Ag_3Ga_5Te_9$ and $Ag_3In_5Te_9$ have received considerable attention lately as potential candidates for several applications as photo-absorbers in solar cells, opto-electronics devices, and photoelectrochemical cells [4], whereas $Cu_3Ga_5Te_9$ [5,6] and $Cu_3In_5Te_9$ [7] are of great interest for thermoelectric applications. As regards to the crystal structure of these $I_3-III_5-VI_9$ compounds, although several studies on the indexing and space group assignation have been reported for various authors from powder X-ray diffraction analysis, some controversy still exists about this subject in these materials (for details, see Table I, where crystals systems, space groups and unit cell parameters for the $I_3-III_5-VI_9$ compounds are listed). In any case, a detailed structural study was conducted.

As observed in this Table, hexagonal, orthorhombic and tetragonal crystal systems have been reported for $Cu_3In_5Te_9$. Recently, in an attempt to analyse its crystal structure, Guedez *et al.* [14] have assigned to this compound the tetragonal space group $I\bar{4}$. However, since incorrect ion distribution and occupancy factors were achieved in this analysis, the stoichiometric composition thus obtained, which is $Cu_{0.924}In_{1.301}Te_{9.545}$, greatly disagrees with the nominal composition $Cu_3In_5Te_9$. In addition, this cationic and anionic distribution derives at a Cu-Te bond distance greater than that of In-Te bond, which gives no chemical sense to this structural model.

For this reason, in order to derive a model that explains well all the X-ray diffraction peaks observed in the powder pattern of this compound, to clarify the discrepancy related to its crystal structure, and to refine it by means of the Rietveld method, a detailed structural analysis of the ordered vacancy compound $Cu_3In_5\square Te_9$ using powder X-ray diffraction was performed.

2. Experimental

Samples of $Cu_3In_5Te_9$ used in this study were prepared by the vertical Bridgman-Stockbarger technique. Stoichiometric mixture of highly pure components of Cu, In and Te (99.999%) were sealed in an evacuated ampoule. Initially, the ampoule was heated from room temperature to 1170 K at a rate of 20 K/h. The molten mixture was then heated to 1370 K at 10 K/h and kept at this temperature for 12 h. To assure a homogeneous mixing the ampoule was agitated peri-

TABLE I. Crystal data for ternary $I_3-III_5-VI_9$ (I= Ag,Cu, III= Ga,In, VI= Se,Te) compounds.

Compound	System	Space group	Unit cell parameters (Å, °)	Ref.
$Ag_3Ga_5S_9$	Tetragonal	$P4$ or $P4mn$	5.759(1), 10.314(3)	[8]
$Ag_3Ga_5Se_9$	Orthorhombic	$Pmm2$	9.767, 5.257, 9.225	[4]
$Ag_3Ga_5Te_9$	Orthorhombic	$Pmm2$	15.94(6), 4.512(4), 7.164(8)	[8]
$Ag_3In_5S_9$	Monoclinic	$P2$ or Pm	10.813(5), 7.661(4), 4.362(1), 91.7(3)	[8]
$Ag_3In_5Se_9$	Tetragonal	$P4$ or $P4mn$	6.714(2), 10.430(4)	[8]
$Ag_3In_5Te_9$	Tetragonal	N. I.*	7.21, 14.57	[9]
	Tetragonal	N. I.	8.738, 7.147	[9]
$Cu_3Ga_5S_9$	Hexagonal	$P6/mmm$	N. I.	[10]
$Cu_3Ga_5Se_9$	Orthorhombic	$Pmm2$	21.947(5), 3.977(1), 5.581(1)	[8]
	Hexagonal	$P6/mmm$	N. I.	[10]
$Cu_3Ga_5Te_9$	N. I.	N. I.	N. I.	-
$Cu_3In_5S_9$	Monoclinic	N. I.	6.6, 8.12, 6.91, 89.0	[11]
$Cu_3In_5Se_9$	Orthorhombic	$Pmm2$	9.767(2), 9.225(5), 5.257(2)	[12]
	Tetragonal	$P\bar{4}2c$	5.7630(4), 11.5370(8)	[13]
$Cu_3In_5Te_9$	Hexagonal	N. I.	8.78, 18.66	[1]
	Orthorhombic	$Pmm2$	12.364(3), 4.374, 11.118(5)	[8]
	Tetragonal	$P4$ or $P\bar{4}mn$	8.738 (3), 7.147(2)	[12]
	Tetragonal	$P\bar{4}2c$	6.185(1), 12.41(1)	[13]
	Tetragonal	$I\bar{4}$	6.1836(2), 12.400(1)	[14]
	Tetragonal	$P\bar{4}2c$	6.1852(2), 12.3633(9)	this work

*N. I. = No information about this item is given in the literature

odically. It was later cooled at 10 K/h to 1090 K, and at 5 K/h to 800 K. The ingot was annealed at this temperature for 120 h. The furnace was then turned off and the ingot cooled down to the room temperature.

The chemical analysis of samples taken from the central part of the ingots, performed by Energy Dispersive X-ray Spectroscopy (EDS), gave representative compositions of Cu: In: Te as 16.58:30.00:53.42 at. percentage, respectively, very close to the 3:5:9 ideal value. There is, however, a slight deficiency of Cu over In (Cu/In ≈ 0.55) and a slight excess of Te over cations (Te/metal ≈ 1.15).

For the X-ray analysis, a small quantity of the sample, cut from the ingot, was ground mechanically in an agate mortar and pestle. The resulting fine powder was mounted on a flat zero-background holder covered with a thin layer of petroleum jelly. The X-ray powder diffraction data was collected at 293(1) K, in $\theta/2\theta$ reflection mode using a Siemens D5005 diffractometer equipped with an X-ray tube (CuKα_1 radiation: $\lambda = 1.54056$ Å; 40 kV, 30 mA). A fixed aperture and divergence slit of 1 mm, a 1 mm monochromator slit, and a 0.1 mm detector slit were used. The specimen was scanned from $10-100^\circ$ 2θ, with a step size of 0.02° and counting time of 10 s. Quartz was used as an external standard. The Bruker AXS analytical software was used to establish the positions of the peaks.

3. Results and Discussion

The X-ray diffractogram of $Cu_3In_5\square Te_9$ shows a single phase. The 2θ positions of the 20 first peaks in the diffraction pattern were introduced into the auto-indexing program Dicvol04 [15], and a tetragonal cell of dimensions $a = 6.186(1)$ Å, $c = 12.365(2)$ Å, were obtained. This cell is similar in magnitude to the parent chalcopyrite structure of $CuInTe_2$, $a = 6.194(2)$ Å, $c = 12.416(4)$ Å [16]. The lack of systematic absence condition $h+k+l$ in the general reflections of the type hkl indicating a P-type cell and rule out the I-type cell of the chalcopyrite structure. In addition, the conditions $hhl : l =$ 2n and $00l : l =$ 2n suggests the extension symbol $P\bar{4}2c$.

A search in the Inorganic Crystal Structure Database (ICSD) [17] showed an early report by Hönle *et al.* [18] of a Cu-poor Cu-In-Se compound β-$Cu_{0.39}In_{1.2}Se_2$, which was solved by single crystal in the space group $P\bar{4}2c$, known as $P-$chalcopyrite structure. The similarity in the space group symbol with our structure gave indications that β-$Cu_{0.39}In_{1.2}Se_2$ structure, with cation distribution: Cu1 in $2e$ (0,0,0); Cu2 in $2b$ (1/2,1/2,1/2); In1 in $2f$(1/2,1/2,0); In2 in $2d$ (0,1/2,1/4), could be a good starting point to construct the initial structural model for $Cu_3In_5Te_9$.

Thus, several models were derived from Hönle's structure by permuting the cations in the available Wyckoff positions.

TABLE II. Models employed for the cation distribution in the Rietveld refinement of the ordered vacancy compound $Cu_3In_5\square Te_9$.

Model	(2e)	(2a)	(2b)	(2c)	(2d)	(2f)	(8n)	R_p	R_{wp}	S
	0,0,0	0,0,1/4	1/2,0,1/4	1/2,1/2,1/4	0,1/2,1/4	1/2,1/2,0	x, y, z			
1	CU1	□	Cu2−In3	–	In1	In2	Te	10.8	12.1	1.9
2	Cu1	□	Cu2−In3	–	In2	In1	Te	7.1	8.5	1.3
3	Cu1	□	In1	–	Cu2−In3	In3	Te	12.8	18.1	2.5
4	Cu1	□	In1	–	In3	Cu2-In3	Te	12.2	18.0	2.5
5	Cu1	□	In2	–	In1	Cu2-In3	Te	18.7	25.1	3.5
6	Cu1	□	In2	–	Cu2-In3	In1	Te	20.2	30.2	4.2
7	Cu1	□	In3	–	In2	Cu2-In3	Te	9.4	10.0	1.6
8	Cu1	□	In3	–	Cu2-In3	In2	Te	11.1	14.6	2.0
9	Cu1	–	Cu2-In3	□	In1	In2	Te	12.0	18.5	2.6
10	Cu1	–	Cu2-In3	□	In2	In1	Te	9.7	10.5	2.7
11	Cu1	–	In1	□	Cu2-In3	In3	Te	12.8	18.1	2.5
12	Cu1	–	In1	□	In3	Cu2-In3	Te	12.2	18.0	2.5
13	Cu1	–	In2	□	In1	Cu2-In3	Te	18.5	25.1	3.5
14	Cu1	–	In2	□	Cu2-In3	In1	Te	20.2	30.1	4.2
15	Cu1	–	In3	□	In2	Cu2-In3	Te	9.9	10.2	1.6
16	Cu1	–	In3	□	Cu2-In3	In2	Te	11.1	14.6	2.0

Cu2 (cation) (foc= 0.333); In3 (cation) (foc= 0.222); Te (anion) : ($x \approx 1/4$, $y \approx 1/4$,$z \approx 1/8$); □ = cation vacancy.

TABLE III. Rietveld refinement results for $Cu_3In_5\square Te_9$.

Molecular formula	$Cu_3In_5\square Te_9$	wavelength (CuKα)	1.54056 Å
Molecular weight (g/mol)	2063.2	data range $2\theta(^\circ)$	10-100
a (Å)	6.1852(2)	step size $2\theta(^\circ)$	0.02
c(Å)	12.3633(9)	counting time (s)	40
c/a	2.00	step intensities	4501
V (Å^3)	472.98(4)	independent reflections	162
Z	0.889 (8/9)	R_p (%)	7.1
Crystal system	tetragonal	R_{wp} (%)	8.5
Space group	$P\bar{4}2c$ (N° 112)	$R_{\rm exp}$ (%)	6.4
d_{calc} (g/cm^{-3})	5.97	R_B (%)	7.8
Temperature (K)	298(1)	S	1.3

$R_{\rm exp} = 100[(\text{N-P+C})/\sum_w(y^2_{\rm obs})]^{1/2}$ $R_p = 100\sum|y_{\rm obs} - y_{\rm calc}|/\sum|y_{\rm obs}|$ $R_{wp} = 100[\sum_w|y_{\rm obs} - y_{\rm calc}|^2/\sum_w|y_{\rm obs}|^2]^{1/2}$ $S = [R_{\rm wp}/R_{\rm exp}]$
$R_B = 100\sum_k|I_k - I_{ck}|/\sum_k|I_k|$ N-P+C is the number of degrees of freedom

Table II shows 16 models tested against the diffraction data by means of the Rietveld refinement method [19], all of which have the Cu^+ cations (Cu1) placed in the origin with Wyckoff position ($2e$): 0,0,0 and Cu2-In3 sharing a position with occupancy factors (foc) 0.333 and 0.222, respectively. Other 16 tests were performed where the Cu^+ cations moved from the origin, and only poor quality Rietveld refinement fits were obtained, and therefore, not presented here.

The Rietveld refinements were carried out using the Fullprof program [20,21]. The angular dependence of the peak Full Width at Half Maximum (FWHM) was described by the Cagliotti's formula [22], whereas peak shapes by the parameterized Thompson-Cox-Hastings pseudo-Voigt profile function [23]. The background variation was described by a polynomial with six coefficients, and the thermal motion of the atoms by one overall isotropic temperature factor. From the figures of merit R_p, R_{wp} and S, it was inferred that the model that best fit the diffraction data is the No. 2. The results of the Rietveld refinement for this model are summarized in Table III. The observed calculated and difference profiles for the final cycle of Rietveld refinements are shown in Fig. 1. Atomic coordinates, isotropic temperature factor, bond distances and angles are listed in Tables IV and V.

TABLE IV. Atomic coordinates, occupancy factors and isotropic temperature factors for $Cu_3In_5\square Te_9$, derived from the Rietveld refinement.

Atom	Ox.	Wyck.	x	y	z	foc	B (Å^2)
Cu1	+1	$2e$	0	0	0	1	0.5(3)
In1	+3	$2f$	1/2	1/2	0	1	0.5(3)
In2	+3	$2d$	0	1/2	1/4	1	0.5(3)
Cu2		$2b$	1/2	0	1/4	0.333	0.5(3)
In3		$2b$	1/2	0	1/4	0.222	0.5(3)
□	-	$2a$	0	0	Â$\frac{1}{4}$	1	-
Te	-2	$8n$	0.2248(8)	0.2547(8)	0.1197(7)	1	0.5(3)

TABLE V. Distance lengths (Å) and bond angles (°) for $Cu_3In_5\square Te_9$.

Cu1-Te	2.570(6)	In1-Te	2.718(6)	In2-Te	2.614(7)
Te^{i}-Cu1-Te	109.4(2)	Te^{ii}-Cu1-Te^{iv}	109.7(2)	Te^{iii}-Cu1-Te^{iv}	109.4(2)
Te^{ii}-Cu1-Te^{iii}	109.4(2)	Te^{iii}-Cu1-Te	109.7(2)	Te-Cu1-Te^{iv}	109.4(2)
Te^{Viii}-In1-Te	107.2(2)	Te^{viii}-In1-Te^{x}	114.0(2)	Te-In1-Te^{x}	107.2(2)
Te^{Viii}-In1-Te^{ix}	107.2(2)	Te-In1-Te^{ix}	114.0(2)	Te^{ix}-In1-Te^{x}	107.2(2)
Te-In2-Te^{v}	x2 109.0(2)	Te-In2-Te^{vi}	x2 115.7(2)	Te-In2-Te^{vii}	x2 103.9(2)

Symmetry codes: (i) 1-x, -y, z; (ii) -y, x, -z; (iii) -x, -y, z; (iv) y, -x, -z; (v) -x, y, 0.5-z; (vi) x, 1-y, 0.5-z; (vii) -x, 1-y, z; (viii) y, 1-x, -z; (ix) 1-x, 1-y, z; (x) 1-y, x, -z.

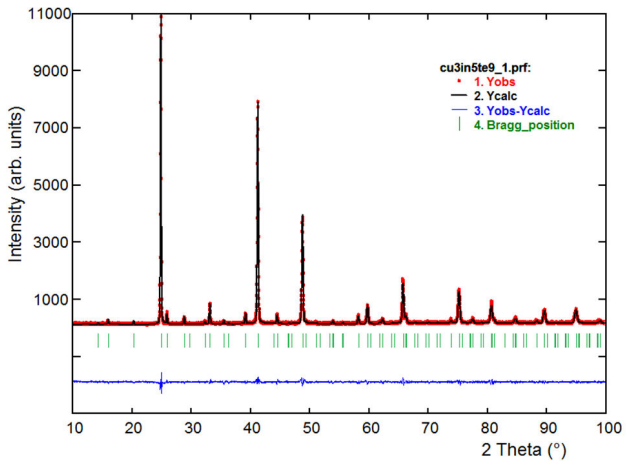

FIGURE 1. Final Rietveld refinement plot for $Cu_3In_5\square Te_9$. The lower trace is the difference curve between observed and calculated patterns. The Bragg reflections are indicated by vertical bars.

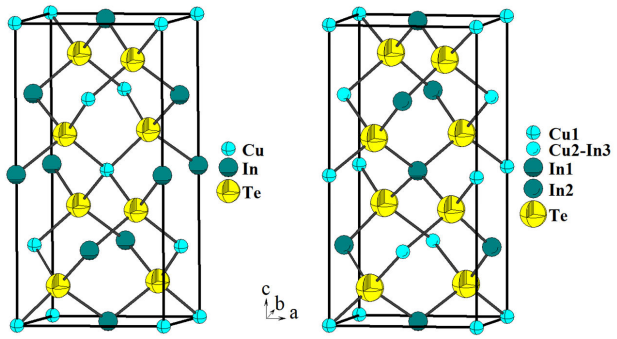

FIGURE 2. Unit cell diagram for the chalcopyrite $CuInTe_2$ ($I\bar{4}2d$) compared with the new $P-$chalcopyrite $Cu_3In_5\square Te_9$ ($P\bar{4}2c$).

$Cu_3In_5\square Te_9$ is an ordered vacancy compound [7], which crystalize in a P-chalcopyrite structure [18], and consists of a three-dimensional arrangement of distorted CuTe4 and InTe4 tetrahedral connected by common faces. In this structure, each Te atom is coordinated by four cations (one Cu and three In) located at the corners of a slightly distorted tetrahedron. In the same way, each cation is tetrahedrally bonded to four anions. This array is expected for adamantane compounds [24]. The unit cell diagram for $Cu_3In_5\square Te_9$ compound, as compared to that of the chalcopyrite $CuInTe_2$ parent, is shown in Fig. 2. It is possible to observe in this figure the In cation and vacancy sites. In the P-chalcopyrite structure, the introduction of additional In cations in the crystal lattice of $CuInTe_2$ produces its "dilution" in the chalcopyrite structure, which leaves the cell volume unchanged.

This behavior was also observed in $CuFeInSe_3$ [25], with composition I-II-III-VI_3, and in the OVC's $Cu_3In_7Se_{12}$ [26] and $Cu_3In_7Te_{12}$ [27,28] with composition I_3-III_7-$\square_2$-VI_{12}. The tetrahedra containing the Cu atoms [mean Te...Te distance 4.20(1) Å] are lightly smaller than those containing the In2 atoms [mean Te...Te distance 4.27(1) Å], In1 atoms [mean Te...Te distance 4.44(1) Å] and (Cu2-In3) [mean Te...Te distance 4.61(1) Å], respectively. The Cu-Te [2.570(6) Å] and In-Te [2.666(7) Å] average bond distances compare quite well with those observed in other adamantine structure compounds such as $CuInTe_2$ [16], $CuTa_2InTe_4$ [29], Cu_3NbTe_4 [30], $CuCo_2InTe_4$ and $CuNi_2InTe_4$ [31], $Cu_3In_7Te_{12}$ [27,28], $AgIn_5Te_8$ [32] and $AgInTe_2$ [33].

4. Conclusions

The crystal structure solution of the semiconductor compound $Cu_3In_5Te_9$ (or $Cu_3In_5\square Te_9$) was resolved in the space group P 2c by the evaluation of different models derived from the $\square$-$Cu_{0.39}In_{1.2}Se_2$ structure against the powder X-ray diffraction data, using the Rietveld method. This compound crystallizes in a $P-$chalcopyrite structure, and is the first structural report on a member of the I_3-III_5 $-$ $\square-VI_9$ semiconductor composition.

Acknowledgments

This work was supported by FONACIT (Grant LAB-97000821).

1. V.I. Tagirov, N. Gakhramanov, A. Guseinov, F. Aliev, G. Guseinov, *Sov. Phys. Cryst*. *25* (1980) 237.
2. B.R. Pamplin, *J. Phys. Chem. Solids* **25** (1964) 675.
3. S.B. Zhang, S.H. Wei, A. Zunger, *Phys. Rev. Lett*. **78** (1997) 4059.
4. N.M. Gasanly, *Mater. Sci. Semicond. Process*. **68** (2017) 213.
5. T. Plirdpring *et al., Mater. Trans*. **53** (2012) 1212.
6. J. Cui, Z. Sun, Z. Dua, Y. Chao, *J. Mater. Chem. C* **4** (2016) 8014.
7. T. Plirdpring, *Adv. Sci. Lett*. **19** (2013) 183.
8. H. Özkan, N.M. Gasanly, I. Yilmaz, A. Culfaz, V. Nagiev, *Tr. J. of Physics* **22** (1998) 519.
9. N.M. Gasanly, *Mod. Phys. Lett. B* **30** (2016) 1650229.
10. N.M. Gasanly, A.G. Guseinov, E.A. Aslanov, S. El-Hamid, *Phys. Status Solidi B* **158** (1990) K85.
11. A.Z. Abasova, L.G. Gasanova, A.G. Kyazimzade, *Inst. Phys. Conf. Ser.* **152** (1997) 87.
12. M. Parlak *et al., Cryst. Res. Technol*. **32** (1997) 395.
13. C. Rincón, S.M. Wasim, G. Marín, J.M. Delgado, J. Contreras, *Appl. Phys. Lett*. **83** (2003) 1328.
14. E. Guedez *et al., Mater. Lett*. **186** (2017) 155.
15. A. Boultif, D. Löuer, *J. Appl. Cryst.* **37** (2004) 724.
16. K.S. Knight, *Mater. Res. Bull*. **27** (1992) 161.
17. Inorganic Crystal Structure Database (ICSD), Gemlin Institute, Kalrsruhe, Germany, (Set 2008-02)
18. W. Hönle, G. Kühn, U.C. Boehnke, *Cryst. Res. Technol*. **23** (1998) 1347.
19. H.M. Rietveld, *J. Appl. Cryst*. **2** (1969) 65.
20. J. Rodriguez-Carvajal, *Physica B* **192** (1993) 55.
21. J. Rodriguez-Carvajal, Fullprof ver. 6.2, Laboratoire Léon Brillouin (CEA-CNRS), France (2018).
22. G. Cagliotti, A. Paoletti, F.P. Ricci, *Nucl. Instrum*. **3** (1958) 223.
23. P. Thompson, D.E. Cox, J.B. Hastings, *J. Appl. Cryst*. **20** (1987) 79.
24. E. Parthé in: J.H. Westbrook, R.L Fleischer (Eds.), *Intermetallic compounds, principles and applications*, (1995), **Vol. 1**, Jhon Wiley & Sons, Chichester, UK.
25. A.J. Mora, G.E. Delgado, P. Grima-Gallardo, *Phys. Status Solidi (a)* **204** (2007) 547.
26. G.E. Delgado, L. Manfredy, S.A. López-Rivera, *Powder Diffr*. **33** (2018) 237.
27. E. Guedez *et al., Phys. Status Solidi (b)* **254** (2017) 1700087.
28. G.E. Delgado, E. Guedez, G. Sanchéz-Pérez, C. Rincón, G. Marroquin, *Materia* (2019) In press.
29. G.E. Delgado *et al., Physica B* **402** (2008) 3228.
30. G.E. Delgado *et al., Chalcogenide Lett.* **6** (2009) 335.
31. G.E. Delgado et al., Mat. Res. **19** (2016) 1423.
32. A.J. Mora, G.E. Delgado, C. Pineda, T. Tinoco, *Phys. Status Solidi A* **201** (2004) 1477.
33. G.E. Delgado, A.J. Mora, C. Pineda, R. Ávila, S. Paredes, *Rev. LatinAm. Metal. Mat*. **35** (2015) 110.